Management of Materials Properties in an Electro-Thermo-Metallurgical Simulation of Quenching Following Inductive Surface Heating

M. Kchaou, D. Durand, and J.P. Sagaspe

A numerical model for simulating quenching following inductive surface heating is proposed. The metallurgical model, which is based on the superposition principle and uses isothermal data, is integrated within a computerized code for heat exchanges (Flux2D) in order to simulate the thermal kinetics at any point on a test piece. The profile of the zones transformed during a rapid cycle can then be computed. This has been made possible by constructing a coupling scheme that considers the interaction effects among heat transfer, magnetic, and metallurgical phenomena. The coupling is based on a new approach that involves separating the physical laws into equation form to describe the physical phenomena and properties of the material. The latter has been investigated in depth in order to manage the properties in a more representative manner by considering the effect of phase transformations on changes in these properties. An illustrative example compares a coupled thermo-metallurgical numerical simulation with experimental results for treated cylindrical test pieces.

Keywords
induction hardening, induction heating, inductive heat modeling, quench modeling

1. Introduction

QUENCH hardening following inductive heating of the surface (QHIHS) involves austenitizing the surface layer of the piece to be treated by heating, then rapidly cooling in order to subject the austenitized layer to martensitic quenching. The principle used for heating the piece is a direct application of Lenz's law combined with the Joule effect. The piece to be treated is placed inside an inductor (solenoid or wound) (Fig. 1). The supply of high-amperage alternating current to the inductor creates a variable magnetic field, usually in the form of a sinusoidal wave. Electromotive induction forces are created in the electrically conductive piece, and currents are induced (Foucault currents). These currents can dissipate a large quantity of heat to the piece (the Joule effect) and rapidly heat the surface of the material.

The induced current density decreases from the surface to the interior of the piece; thus, the energy is transferred mainly to the surface of the piece. This phenomenon is known as the "skin effect" and is highly dependent on the properties of the materials and the frequency used. Since the heating takes place over a very short period of time, heat conduction is limited, and the heating effect occurs in the outer layer.

The cooling must be sufficiently rapid to transform the austenitized zone into martensite, leaving only a low residual austenite content. The high temperature differences produced by the treatment, combined with the volume variations related to the phase transformations (principally martensitic transformation), result in a residual stress field in the treated piece. This residual stress field is usually characterized by high compressive stresses on the surface.

Figures 2(a) and (b) show the changes in mechanical properties relating to this zone. QHIHS is commonly used in the engineering industry to harden and prestress components and to improve fatigue strength.

Compared to alternative processes, such as case hardening and nitriding, the advantages of QHIHS are short treatment cycle times and the ease with which it can be automated. It can thus be integrated more successfully into a flexible production line.

However, the complex nature of the treatment, its rapidity, and the difficulties associated with measuring physical variables (current, temperature, etc.) have hindered its development. Therefore, numerical simulation of the phenomena governing the process is of particular interest. In this paper, the phenomena that can be recreated using existing software pro-

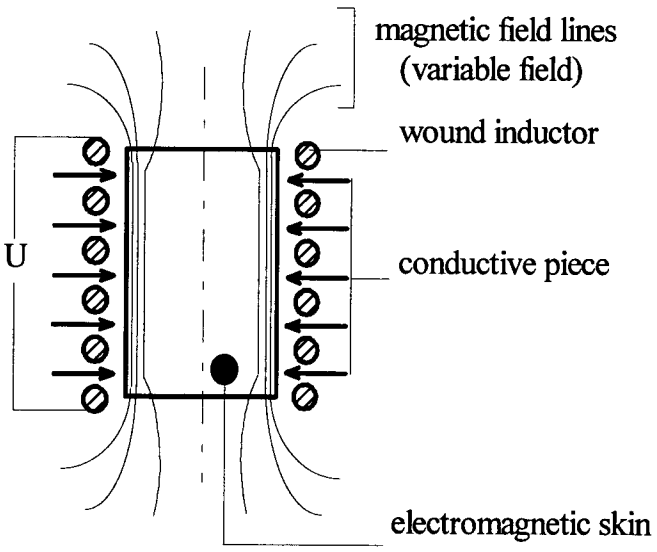

Fig. 1 Principle of inductive heating

M. Kchaou, IPEIS, Route Menzel Chaker km 0, 5, B.P. 805 code 3000 Sfax, Tunisie; **D. Durand** and **J.P. Sagaspe,** ENSAM-Bordeaux, Esplanade des Arts et Métiers, 33405 Talence, France.

grams such as Flux2D are analyzed, and then a metallurgical model is proposed for calculating phase transformations.

2. Phenomena

This study involves two varied yet associated fields of engineering science: electromagnetism and heat transfer.

2.1 *Electromagnetism*

When an inductor is supplied with variable alternating current, a variable magnetic field is created around the inductor. Any electrically conductive element in this magnetic field is affected by electromotive induction forces, and current is induced.

The distribution of the currents and the energy dissipated in the piece can be determined exactly using Maxwell's equations, which describe the fundamental laws of electromagnetism:

$$\text{rot}\ \vec{E} = -\frac{\partial \vec{B}}{\partial t}$$

$$\text{div}\ \vec{B} = 0$$

$$\text{rot}\ \vec{H} = \vec{j} + \vec{j_0}$$

$$\text{with}\ \vec{j} = \sigma\vec{E} \rightarrow (4) \rightarrow \text{and} \rightarrow \sigma = \frac{1}{\rho}$$

where **E** is electric field, **H** is magnetic field, **B** is magnetic induction, **j** is current density in the piece, $\mathbf{j_0}$ is current density in the inductor, σ is material conductivity, and ρ is electrical resistivity.

In the conductive piece, the magnetic induction **B** is a function of the magnetic field, in accordance with:

$$\vec{B} = \mu\vec{H}$$

where the coefficient μ indicates the permeability at each point in the material. Since the parameters ρ (electrical resistivity) and μ (permeability) are functions of the temperature and the metallurgical phases, solving Maxwell's equations is a complicated process.

2.2 *Heat Transfer*

Understanding the thermal changes that take place during heat treatment requires solving the heat equation (Fourrier's equation), which is written in a reduced form for an isotropic material:

$$\text{div}\ [\lambda\ \text{grad}\ (T)] + \dot{q} = \rho Cp\frac{\partial T}{\partial t}$$

where T is temperature, λ is thermal conductivity, ρ is density, Cp is specific heat, and $\dot{q}$ is internal heat generated by the Joule effect and structural transformation.

Modeling the heat transfers between the piece and the surrounding environment, and the effect of heat sources, is essential to determination of the thermal history of the piece. Neuman's nonhomogeneous conditions are generally used for heat treatments:

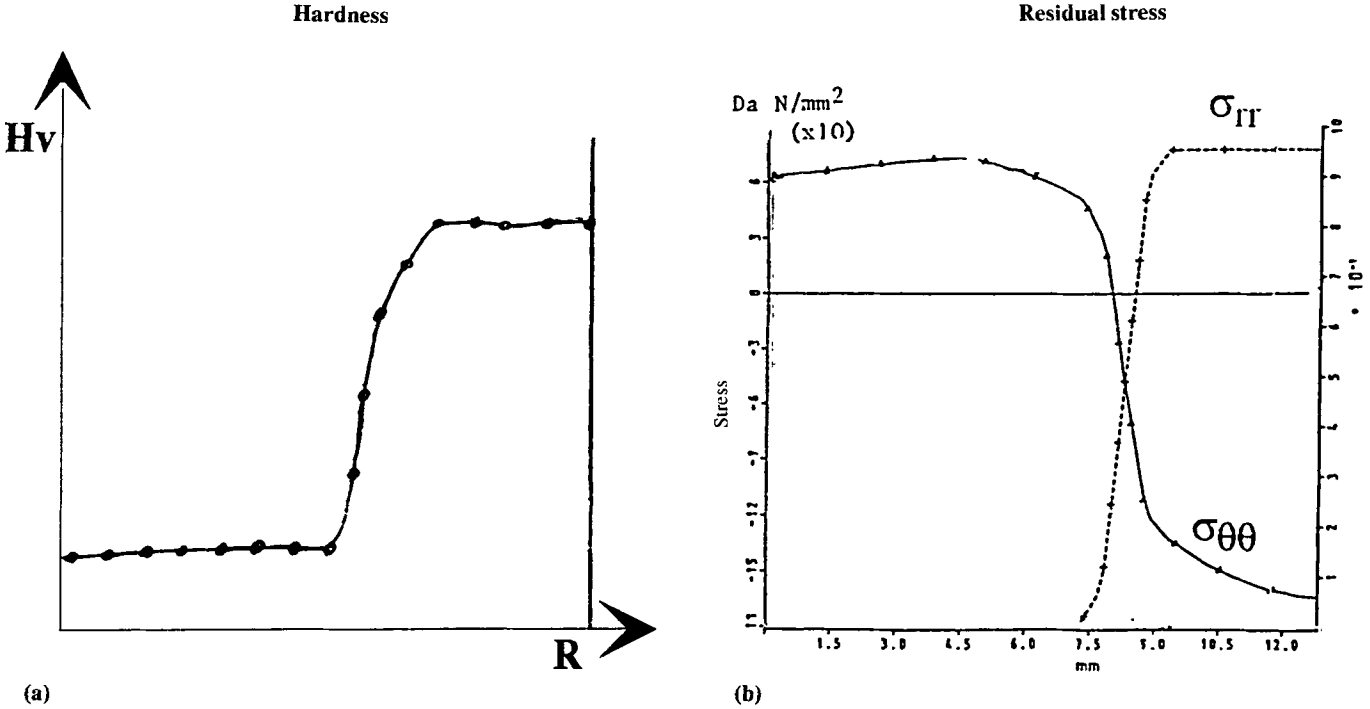

Fig. 2 (a) Hardness changes after surface quenching. (b) Changes in radial and circumferential stresses after surface quenching

$$k\frac{dT}{dn} = -FH - h(T - T_a) - \varepsilon\sigma(T^4 - T_a^4)$$

where k is calorific conductivity, FH is flow of heat provided by the surroundings, T_a is ambient temperature, n is the normal to the surface, ε is emissivity of the surface, and σ is Stephen's constant [5.67×10^{-8} W/(m^2·K^4)].

The main problem is then the determination of the heat-transfer coefficient h, which is a nonlinear function of the surface temperature T and the shape of the heat-exchange surfaces. These equations are satisfactorily solved by various software programs (see, for example, Ref 1 and 2)—particularly by Flux2D, developed by the electrotechnical laboratory at the ENSIEG in Grenoble, France. It can be used to analyze electrical, magnetic, and thermal phenomena and is based on the finite-element method in a steady or dynamic state. It also can be used to calculate and visualize physical variables required by engineers for components in two dimensions or simple three-dimensional pieces through generating shapes by rotation for materials with linear or nonlinear isotropic or anisotropic characteristics.

3. Modeling Metallurgical Transformations

Figure 3 diagrams the metallurgical phenomena involved in surface heat treatment. The thermal cycle can be divided into two stages: heating and cooling. The purpose of the heating stage is to austenitize the steel on the surface of the component to a given depth. The purpose of the cooling stage is to subject the previously austenitized zone of the component to a martensitic quenching.

3.1 *Heating*

Analysis of metallurgical factors as one of the phenomena that govern the quenching process after inductive surface heating has rarely been dealt with in the literature. One exception is the Nancy Mining School (Ref 3), which used a very fast heating technique (laser) comparable to that of inductive heating.

For a tempered quenched structure, the result of these transformations is the presence of the following structures:

- From ambient temperature to Ac_1 temperature (the start of austenitization), the initial structure may be considered unchanged.
- From Ac_1 to Ac_3 temperature, nonhomogeneous austenite is formed, which exists concurrently with the residual initial structure.
- From Ac_3 up to Ac_c (the boundary between nonhomogeneous and homogeneous austenite), homogenization of the austenite occurs after the existing carbides have dissolved.
- Above Ac_c, because the austenite is homogeneous, the austenitic grain size increases with the austenitization temperature, T_{max} (Fig. 3).

In the zone for which T_{max} is less than Ac_1 and when the initial structure is quenched and then tempered, the effect of the second tempering must be considered in terms of the properties of the initial structure.

The initial data available for the heating stage are continuous and isothermal temperature-time-austenitization (TTA) curves for the steel under consideration. In the treated zone, the thermal kinetics at the start of heating affect the Ac_1 temperature and require a coupled, thermo-metallurgical calculation in order to determine this point. In practice, however, it is observed that:

- Within this zone and temperature range, the rates at which temperature increases are relatively linear.
- Small variations in the thermal cycle affect the Ac_1 temperature to a very limited extent.

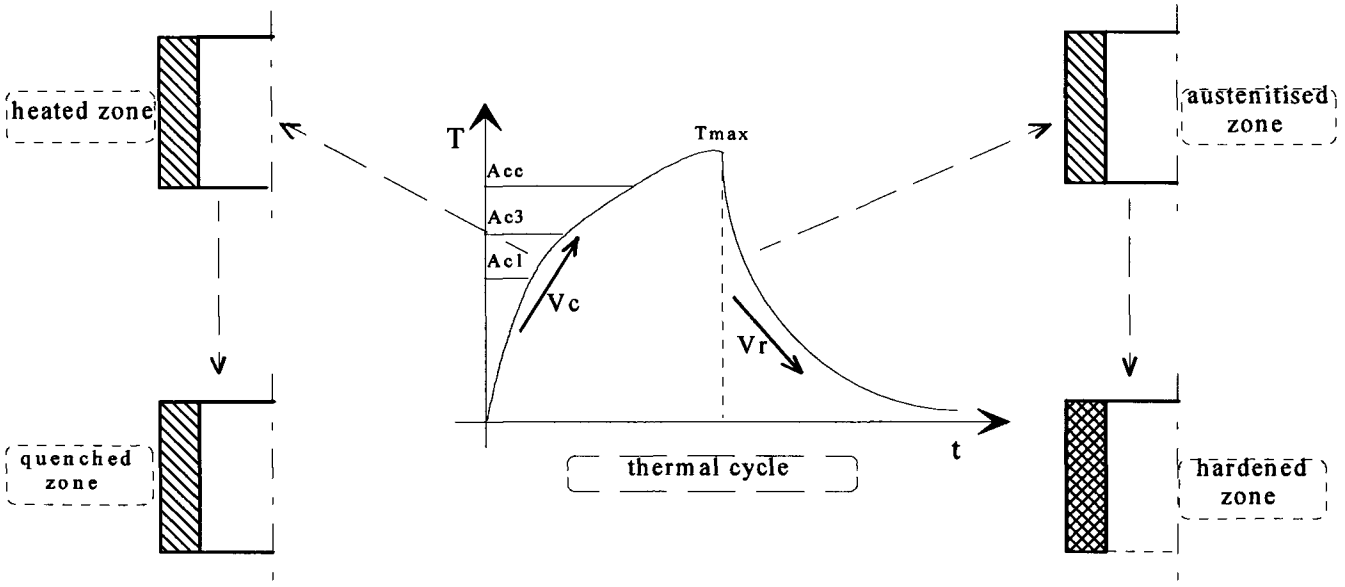

Fig. 3 Metallurgical phenomena during surface heat treatment

3.2 *Modeling Metallurgical Transformations between Ac_1 and Ac_3*

In this twin-phase zone, determination of the amounts of phases present and the chemical composition of the austenite, particularly its carbon content, is necessary for determination of the M_s point and the mechanical properties of the aggregate. In this region, a method is used based on the breaking down of the thermal cycle into discrete, isothermal steps. These step increments enable monitoring of changes in the austenite during heating.

3.2.1 Calculating the Volume Fractions of Austenite

The fraction of austenite formed is calculated using the laws that govern the growth of austenite during isothermal transformations. Several formulas have been proposed (Ref 4). Avrami's law appears to be best suited for describing this change since it offers a good compromise between the physical phenomena and the experimental parameters. It is expressed as:

$$y_k = 1 - e^{(-b_k t^{n_k})}$$

where y_k is the fraction of new phase k, t is time, and b_k and n_k are two temperature-dependent parameters.

3.2.2 Calculating the Isothermal Coefficients (b_k, n_k)

First, the parameters b_k and n_k of Avrami's equation must be determined at a temperature T_i. Thus:

$$\ln(1 - y) = -b_k t^{k_k}$$

Based on the isothermal TTA diagram, three zones (Fig. 4) may be envisaged in order to determine the required data:

- *Zone 1:* $y_d = 5\%$; y_f is calculated by referring to the equilibrium diagram.
- *Zone 2:* $y_d = 5\%$; $y_f = 95\%$
- *Zone 3:* y_d is to be calculated since the austenite fraction at the start of the isothermal transformation is not known.

The austenite fraction varies exponentially with temperature, so this variation can be considered to follow the same model as that proposed by Avrami in order to determine the volume fractions at each temperature. Thus:

$$v = 1 - e^{(-l \cdot T^m)}$$

where v is volume fraction of formed austenite, T is temperature, and l and m are parameters that depend on the phase transformation points. The calculation of l and m is simplified if the fractions at two points corresponding to the start and end of transformation are known.

3.2.3 Calculating the Transformation Progress (y)

The volume fraction of austenite formed after a time t is equal to the sum of the volume fractions formed after each step time (Δt). This approach is the basis for a method that uses the principle of superposition and involves adding the fraction of austenite formed during a step Δt to the fraction that is already formed at a time t. The fraction of austenite formed at a time $t + \Delta t$ is thus obtained up to the end of the heating cycle.

The thermal cycle provided by the thermal calculation software (Flux2D) is broken down into discrete time steps (at constant temperature) lasting Δt and into temperature steps that follow the volume isofraction lines (constant volume fraction of the formed phase) (Fig. 5). This breakdown is made necessary by the fact that temperature changes that do not follow the volume isofraction lines result in a variation of the phase content formed. This variation becomes more significant in the pearlitic transformation zone (the growth of austenite in pearlite is very rapid).

3.2.4 Calculating the Positioning Time for the Steps (t')

The volume fraction of austenite formed at the end of step i is considered to be y_i. In order to move onto the next step, a positioning technique is used that respects the temperature variation following the isovolume lines. An equation of the following type is used:

$$t'_{i+1} = t'_i + \left[\frac{\alpha\left[\frac{t_f - t_d}{Ac_1 - Ac_3}\right]}{1 + \alpha\left[\left[\frac{t_f - t_d}{Ac_1 - Ac_3}\right]\right]} \right] \cdot \Delta t$$

where α is the angle formed by the tangent to the isofraction line, t_d is time at the start of the transformation corresponding to Ac_1 (in seconds), t_f is time at the end of the transformation corresponding to Ac_3 (in seconds), Δt is step time, and t'_i is time at the start of step i.

3.2.5 Calculating the Volume Fraction Formed

After all the required parameters (b_i, n_i, t'_i) are obtained, an Avrami equation of the following form results:

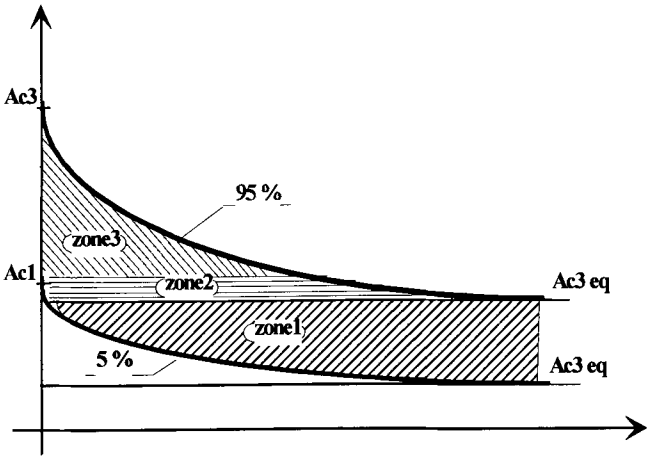

Fig. 4 Distribution of the zones used to calculate Avrami's coefficients

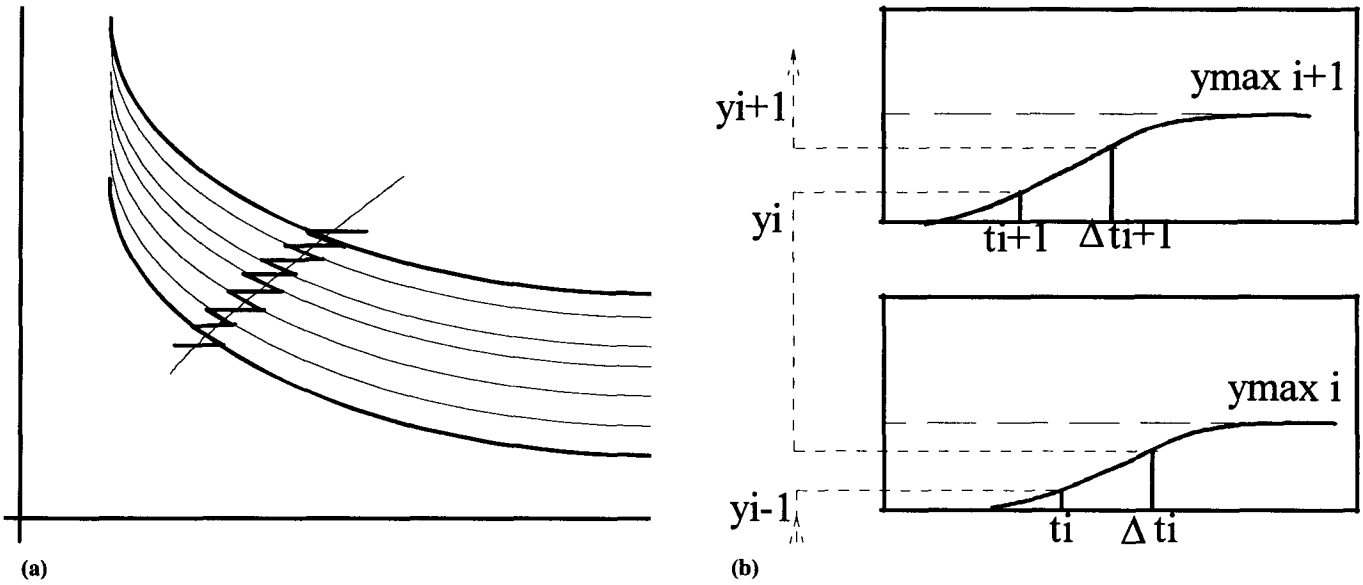

Fig. 5 (a) Principle of breaking down the thermal cycle. (b) Calculation process for phase transformation progression

$$y_{i+1} = (y_{\max})_{i+1}\left[1 - e^{[-b_{i+1}(t'_{i+1} + \Delta t_{i+1})^{n_{i+1}}]}\right]$$

where $(y_{max})_{i+1}$ is the maximum volume of the phase formed at a temperature T_{i+1} for the step $i+1$. The term y_{max} can be determined in two ways:

- By calculation using the Fe-C equilibrium diagram
- Experimentally via tests conducted at constant temperature (T_i) that continue until a stable structure is obtained

If the maximum volume is taken to be the multiplying fraction, then the case of partial phase transformation may be considered, and the maximum heating temperature during treatment will be between Ac_1 and Ac_3—the start and end of transformation, respectively.

3.3 *Modeling Transformations between Ac_3 and Ac_c*

For a given heating rate, the austenite homogenization boundary can be determined either by using continuous TTA diagrams or by calculating the change in the carbon content between Ac_3 and Ac_c, since the change in the carbon content in the austenite becomes a function of temperature. Empirical relationships are used to calculate this parameter, based on the modeling work of Fritsch and Bergmann (Ref 5) and expressed in the form of polynomials.

3.3.1 Austenitic Grain Size

Above Ac_c, the size of the austenitic grain starts to increase. This enlargement is calculated by breaking down the thermal cycle into isothermal steps.

In order to take into consideration the effect of austenitic grain size on metallurgical behavior, the model developed by Ikawa et al. (Ref 6) was chosen. This model describes the growth of austenitic grains during a thermal cycle, which is represented by:

$$D^a - D_0^a = k_0 \sum_i \Delta t_i e^{-Q/RT_i}$$

where D and D_0 are the grain size at time t and the initial grain size, respectively; a and k_0 are positive constants; Q is the apparent activation energy; and R is the ideal gas constant. Use of this equation requires knowing both the initial austenitic grain size at the start of austenitization (D_0 in microns), either taken from the literature or determined experimentally, and the values of the constants in the equation (normally the same as those proposed in the literature, i.e.: $a = 4$, $k_0 = 2.969 \times 10^{15}$ mm^2/min, and $Q = 1.269 \times 10^5$ cal/g atom).

3.3.2 Calculation of M_s

The M_s temperature is calculated as a function of the austenite state. If the austenite is nonhomogeneous (the temperature reached during heating is less than the Ac_c homogenization boundary), the model takes into consideration an M_s temperature that is a function of the carbon content. In this case, two temperatures must be determined:

$$M_{s\ Dark} = M_0 + h(\%C_{Aust\leftarrow Fe} - \%C_{steel})$$

$$M_{s\ Light} = M_0 + h(\%C_{Aust\leftarrow Pe} - \%C_{steel})$$

where the coefficient $h = -423$ (Ref 7). The M_0 temperature is determined from a dilatometric test.

If the austenite is homogeneous, M_s is calculated as a function of the austenitic grain size and is written in the form:

$$M_s = \sum_{n=0}^{n} (b_n D^n)$$

where b_n is the n-order coefficient of the polynomial, and D is the grain size at the end of heating. For a martensitic transformation, the critical quenching rate must be determined using continuous-cooling-transformation (CCT) curves to define the critical velocities associated with each metallurgical phase.

3.4 *Cooling*

The literature describes how austenite can undergo various transformations during the cooling period depending on the velocity V_c (cooling velocity). For a hardening treatment, a martensitic structure is desired whose mechanical characteristics (hardness, fracture strength, etc.) meet specific requirements. The limitation of the model in terms of a martensitic transformation is justified by two considerations. First, the cooling velocities in surface quenching are generally very high, because:

- The zones that are to be cooled are thin and near to the cooling system.
- Heat exchange at the surface is by forced convection.
- The core of the component, which is colder, provides additional cooling of the treated zone.

Second, the required structure in the treated zone must be free from bainite and necessarily from ferrite and pearlite. In the modeling described here, only the formation of martensite is envisaged, with a certain content of residual austenite that is unavoidable if there is no subsequent heat treatment.

In the time interval between T_{max} and M_s, the austenitic structure cools with no metallurgical transformation if the velocity is greater than the previously calculated critical velocity. In the time interval between M_s and ambient temperature, the structure obtained consists of a mixture of two phases: austenite and martensite. When the temperature falls, martensite is formed at the expense of austenite. The martensite percentage is calculated by (Ref 8):

$$y_m = \{1 - e^{[-A_m(M_s - T)]}\}$$

where y_m is the proportion of martensite formed at time t; M_s is the temperature at the start of the martensitic transformation; and A_m is a material parameter, normally constant.

4. Coupled Phenomena

An analysis of the literature indicates that the effect of some of these interactions is negligible in terms of the accuracy of the results and thus can be ignored. Figure 6 shows an initial calculation diagram. In the left-hand block of the diagram are grouped the phenomena that require equations to be solved and that provide information about the physical laws. The right-hand block concerns the treatment of the properties of the materials.

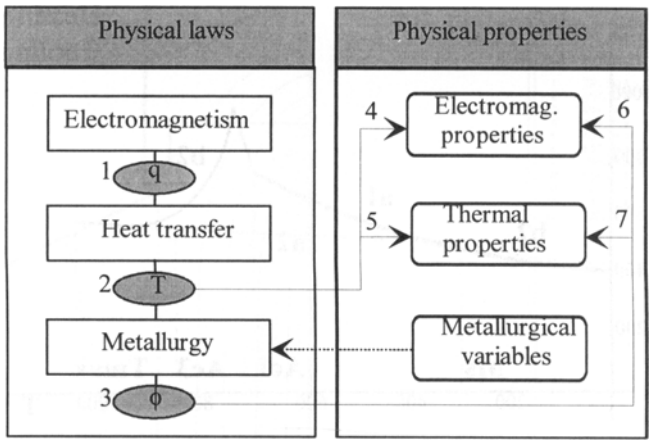

Fig. 6 Initial calculation diagram

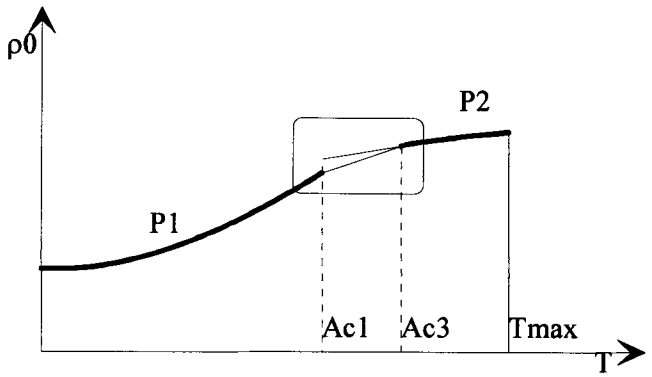

Fig. 7 Changes in electrical resistivity as a function of temperature

The electromagnetic properties of the material are taken into consideration during heating. During measuring, it seems that the electromagnetic values vary sharply with the phase changes. In order to simulate the process with the greatest precision, these values must be corrected as a function of the Ac_1 and Ac_3 temperatures—the start and end of the formation of austenite during heating, respectively. These temperatures at the start and end of the austenitization must be calculated with the help of a metallurgical model. The behavioral models for these properties are illustrated in the following sections.

4.1 *Electrical Resistivity* (ρ_0)

Figure 7 shows changes in electrical resistivity as a function of temperature.

4.2 *Heat Capacity (Cp)*

The metallurgical-thermal coupling is involved in relation to the release of "latent heat." This quantity of heat is an additional internal source in the heat equation during an allotropic transformation. In order to simplify the computing, a very common method is to combine the latent heat with the specific heat

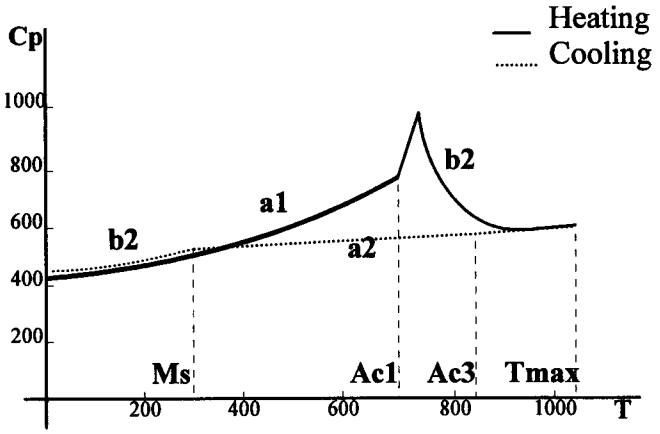

Fig. 8 Changes in heat capacity on heating and cooling

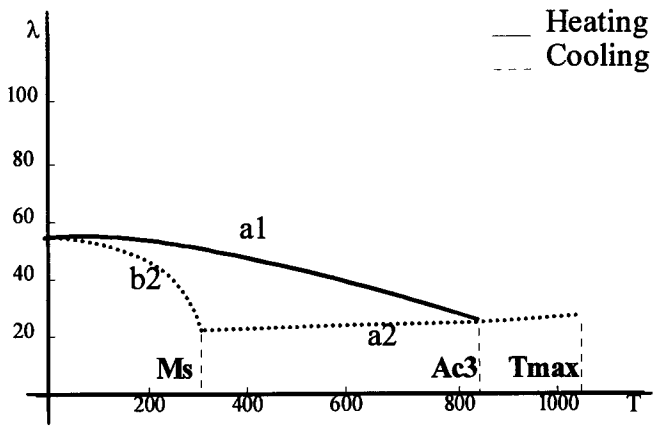

Fig. 9 Thermal conductivity model

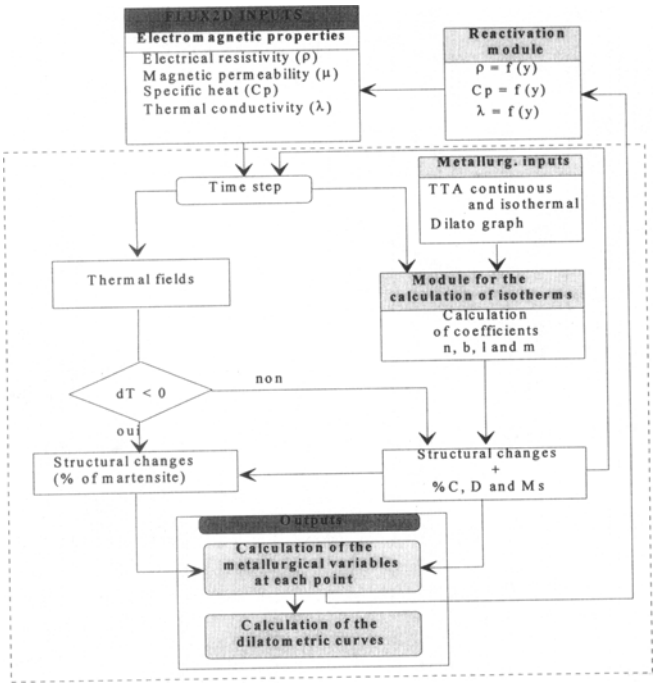

Fig. 10 Flow diagram of the coupled thermal-phase transformation calculation on heating and cooling, and calculation of the dilatometric curves

capacity of the material to produce an equivalent specific heat capacity. This method was adopted, since it enables the latent heat to be taken into account directly in Flux2D.

Our proposed model is shown in Fig. 8. It is valid for a thermal cycle that includes heating and cooling, with the position of the peak varying according to the positions of Ac_1 and Ac_3. For the cooling stage, the position depends on the M_s point.

4.3 *Thermal Conductivity*

Thermal conductivity is greatly influenced by temperature and the existing phase. In order to describe the change in thermal conductivity during a rapid thermal cycle, a model was used that included three zones of temperature variation (Fig. 9).

4.4 *Flow Diagram of the Coupled Calculation*

The flow diagram in Fig. 10 shows the stages in the metallurgical calculation coupled with the magneto-thermal calculation and specifies all input data. The calculation provides information about the changes in temperature and the kinetics of the various phase transformations at all points in the heating and cooling stages. Based on the calculation of the metallurgical variables, the dilatometric curves are calculated using the model that we have developed.

5. Thermal and Metallurgical Simulations

In order to carry out these calculations, the following data were used:

- The physical properties (ρ, λ, and *Cp*) of the treated steel are those described earlier.
- The metallurgical properties are read off the dilatometric graphs for the tempered quenched state.
- The shower quenching effect is modeled by a surface heat-exchange coefficient, *h*, as a function of temperature. These values were supplied by the company SEAT and are based on temperature readings. The change in this coefficient is given in Fig. 11.
- The voltage is obtained by taking measurements at the inductor terminals using the circuit connected to the generator passing via the test bench.

The simulations were performed by carrying out coupled magnetic, thermal, and metallurgical calculations. Coupling with metallurgy was carried out automatically by taking into account the change in the electromagnetic-thermal properties of the material.

5.1 *Simulating Heating*

The calculation was made for a cylindrical test piece. Figure 12 indicates the isothermal surfaces at the end of the heating stage; the maximum temperatures inside the cylinder change slightly during cooling.

In order to take into account the shower lag, the thermal calculation was continued without including the source of internal

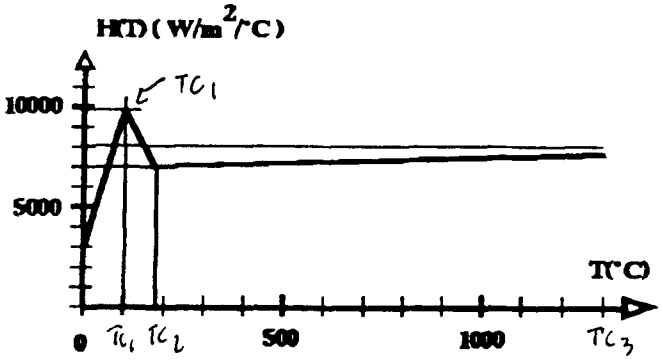

Fig. 11 Change in the coefficient h as a function of temperature

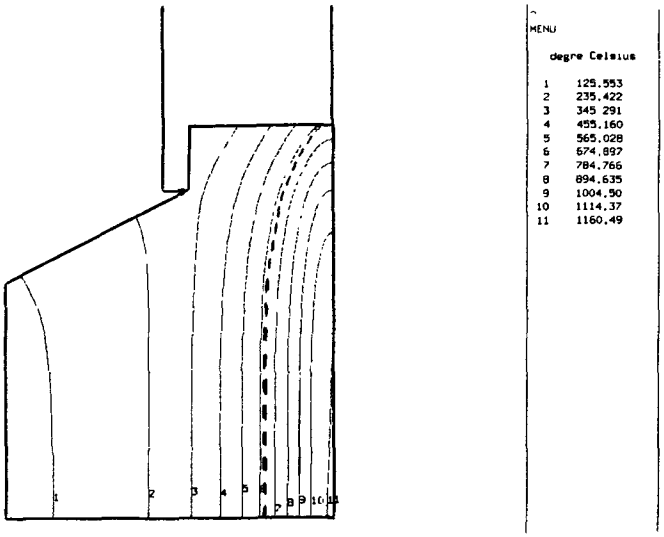

Fig. 13 Isothermal curves at the end of the heating stage. Heating time, 1.41 s; maximum temperature, 1228 °C

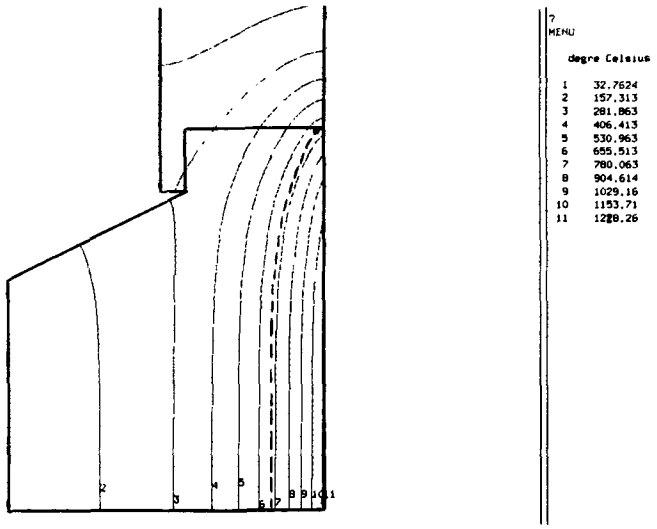

Fig. 12 Isothermal curves at the end of the heating stage. Heating time, 1.41 s; maximum temperature, 1228 °C

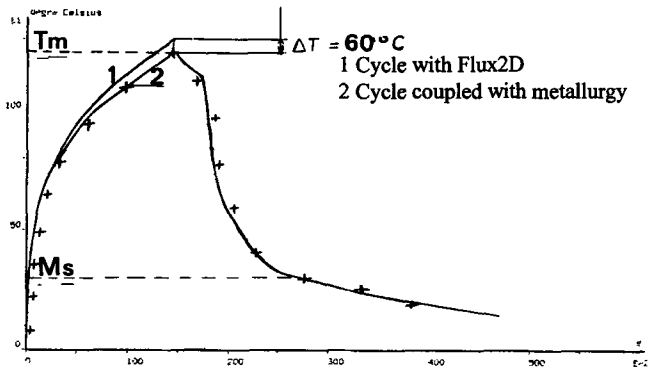

Fig. 14 Comparison of thermal cycles when calculated both coupled with and not coupled with metallurgy

heat (the generator was switched off) and with the limiting radiation conditions. Figure 13 shows the results obtained after a 0.35-s quench. The results illustrate the importance of heat conduction on the cooling of the austenitized zone. The thermal cycle can be deduced from these calculations at the point on the surface that has been compared with the measured cycle.

The same thermal cycle calculated by Flux2D was compared with the cycle obtained above by integrating the modulus of the phase transformations. The difference in corresponding maximum temperatures is approximately 60 °C for this test piece (Fig. 14).

5.2 *Simulating Cooling*

For this period in the thermal cycle, the percentage of austenitic phase that transforms into martensite during cooling was calculated in order to compare the quenched depth, calculated to the 50% formed martensite level, with the measured depth. The martensite isofractions contours are shown in Fig. 15.

The calculated and measured depth values agreed well for the central part of the test piece of length L_1. At the ends, the measured depth was greater than the calculated value in all three cases. This phenomenon is probably due to the thermal resistance between the test piece and the support, which is not taken into account in the calculation.

5.3 *Simulation Based on Data in the Literature*

The calculation was carried out using a cylindrical test piece in annealed XC42 steel in order to simulate the change in the transformation kinetics of the austenite. The change in the austenite content was calculated based on data obtained from the literature using two methods:

- The first method involves breaking down the thermal cycle into steps, and thus ignoring the variation in the volume fraction when the temperature changes from one step (i) to another ($i + 1$) (INPL stair method).
- The second method involves correcting the volume fraction at each step in the calculation (volume isofractions method). This model was selected for the metallurgical calculation.

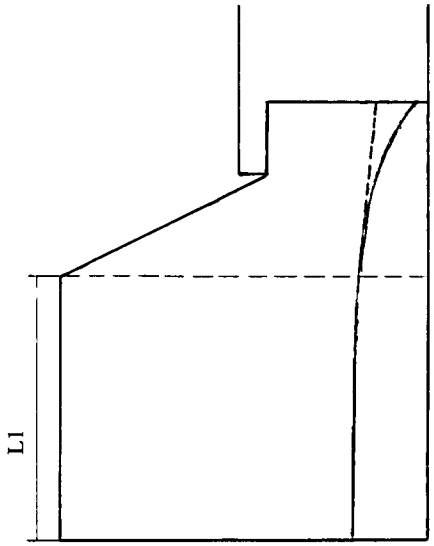

Fig. 15 Contour of the calculated and measured quench depth. Heating time, 1.41 s; maximum temperature, 1228 °C. — Calculated quench-depth (50% of martensite); ... Measured quench depth

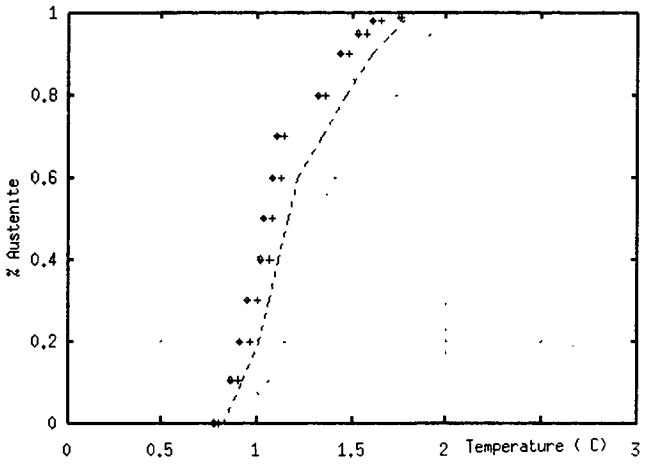

Fig. 16 Comparison of the measured transformation kinetics with those calculated by both methods (Ref 9). ◆ Experimental points 1; + Experimental points 2; ... Stair method; --- Volume isofraction method

Figure 16 compares the measured transformations kinetics with those calculated by both methods. It was observed that the correction of the volume fractions improves the accuracy of the calculation of the residual austenite content in the hardened zone (Ref 10).

6. Conclusions

The various validations carried out confirmed that the various phenomena and the various physical variables of the material must be considered, as precisely as possible, in order to be able to determine the calculated metallurgical transformation kinetics that simulate the actual kinetics. Therefore, the fact that the support/piece interface was viewed as a thermally perfect contact strongly influenced the calculation of the quenched depths at the ends of the test piece. To obtain greater accuracy, a contact resistance must be introduced between the piece and the support, which may then be modeled in the Flux2D program by a thin material with an appropriate resistance. In the same way, the fact that the metallurgical calculations were not coupled with the mechanics of the system (validation of M_s as a function of the stress level) is a major source of inaccuracy in the calculation of the residual austenite content in the hardened zone (Ref 10).

Throughout this paper, a partial validation has been performed concerning the thermo-metallurgical results, which represent an important stage in the predetermination of stresses. This stress calculation requires knowing the mechanical properties of heating and cooling. In the latter case, we have planned to adopt a technique that enables the characteristics of the material to be determined at different temperatures.

Measurement of the residual stresses will be carried out on the cylindrical test piece used in the thermo-metallurgical validation. Plans have been made to measure the surface stresses in the hardened zone using the x-rays method and, since the test piece is geometrically simple, using the SACHS method for the central part of the piece.

References

1. SYSWELD, uses FEM to analyze manufacturing processes involving metallurgical phase changes, Manuel de présentation de fonctionnement du logiciel, Rev. A. Framasoft + CSI, Groupe Framatome, France, 1992
2. Flux2D, Analyse des dispositifs électriques, magnétiques et thermiques par la méthode des éléments finis, CEDRAT S.A., Meylan, France, 1992
3. D. Farias, "Traitement thermique laser de l'acier XC42 et modélisation des transformations de phases en cycles rapides au chauffage et au refroidissement," Thesis, INPL, Nancy, France, July 1991 (in French)
4. F.M.B. Fernandes, "Modélisation et calcul de l'évolution de la température et de la microstructure au cours du refroidissement continu des aciers," Thesis, INPL, Nancy, France, April 1985 (in French)
5. H.U. Fritsch and H.W. Bergmann, "Influence of the Carbon Diffusion during Laser Transformation Hardening—Numerical Simulation and Experimental Verification," presented at Scientific Laser—European Scientific Laser Workshop on Mathematical Simulation, 1989
6. H. Ikawa, S. Shin, H. Oshige, and H.Y. Mekuchi, Austenite Grain Growth during Thermal Cycle in Steels, *Trans. Jpn. Weld. Soc.*, Vol 5 (No. 46), 1977, p 271-278
7. K.W. Andrews, Empirical Formulae for the Calculation of Same Transformation Temperatures, *J. Iron Steel Inst.*, 1965
8. D.P. Koistinen and R.E. Marburger, A General Equation Prescribing Extent of the Austenite-Martensite Transformation in Pure Fe-C Alloys and Plain Carbon Steels, *Acta Metall.*, Vol 5 (No. 7), 1959, p 59-60
9. M. Kchaou, "Contribution à la prédétermination des états structuraux et des contraintes résiduelles après trempe superficielle par induction," Thesis, ENSAM-Bordeaux, France, Jan 1995 (in French)
10. A. Constant, G. Henry, and J.C. Charbonnier, Principe de base des traitements thermiques thermomécaniques et thermochimiques des aciers, PYC Edition, France, 1992 (in French)